Identification of Altered Potassium Channels for Drug Repurposing in Long COVID Patients

John P. George[1,2], Kiran Bharat Gaikwad[1,2], Jyoti Sharma[1,2]*

[1]Manipal Academy of Higher Education, Manipal, Karnataka 576104, India

[2]Institute of Bioinformatics, International Technology Park, Bangalore 560066, India

***Corresponding author.** Dr. Jyoti Sharma, Institute of Bioinformatics, International Technology Park, Bangalore 560066, India. E-mail: jyoti@ibioinformatics.org

Keywords: Post-COVID conditions, transmembrane proteins, immune system, drug repurposing, viral infection, channelopathies, ion channels, cell membrane

Abstract:

Long COVID (LC) is a complex condition characterized by persistent, chronic multisystem manifestations, with a significant proportion of patients exhibiting neurological symptoms. Human ion channels (HICs), particularly potassium channels, are abundantly expressed in the nervous system and linked to key metabolic processes, making them potential candidates for understanding LC pathophysiology and drug repurposing. Meta-analysis of RNA-Seq datasets from COVID-19 recovered and LC patients was performed to identify altered HICs in LC. Differential gene expression analysis, functional enrichment analysis, and weighted gene co-expression network analysis (WGCNA) were performed to uncover key genes, pathways, and co-expression modules consisting of HICs, lipid metabolism-, and immune signaling-related genes. Drug-gene interaction analysis was performed to identify approved drugs targeting potential HICs. A total of 715 dysregulated genes, including eighteen HICs were identified, among which seven were potassium channels. Three significant modules containing HICs, lipid metabolism-, and immune signaling-related genes were identified and found to be associated with antigen processing and presentation, complement and coagulation cascades, and cytokine-related pathways. Approved drugs targeting *KCNA6*, *KCNJ10*, *KCNN3*, and *KCNH4* were identified. With further experimental validation, these dysregulated potassium channels, supported by their co-expression networks and pathway associations, may act as potential candidates for drug repurposing in LC patients.

1 Introduction

Six years after the COVID-19 pandemic, long COVID (LC) continues to be a significant concern among individuals with a history of SARS-CoV-2 infection. It affects a substantial proportion of COVID-19 survivors worldwide, presents with overlapping symptom subtypes and is more likely to occur in individuals with severe disease, comorbidities, and certain demographic risk factors (1). It is primarily characterized by persistent fatigue, brain fog, dyspnea, chest pain, palpitations, and other multisystem manifestations involving the neurological, respiratory, cardiovascular, and musculoskeletal systems (1), (2). These symptoms are thought to arise from multiple overlapping mechanisms, including viral persistence, immune dysregulation, chronic inflammation, microvascular dysfunction, autonomic imbalance, and reactivation of latent viruses (2).

Significant alterations in host gene expression are induced during COVID-19 infection, primarily dysregulating immune response genes, proinflammatory cytokines, and interferon (IFN) pathways (3). Emerging studies using transcriptomic profiling have revealed persistent alterations in gene expression associated with immune dysregulation, inflammation, and metabolic imbalance in affected individuals with elevated proinflammatory cytokines, including interleukin-6 and tumor necrosis factor-α, and altered T and B-cell profiles (4). Elevated expression levels of IFNs in patients with severe COVID-19 have been reported to decline over time in LC patients, suggesting cytokine exhaustion as a possible driver of LC (5). We hypothesized that more integrated transcriptomic analysis is required to elucidate the interconnected molecular networks driving LC pathophysiology that could also provide therapeutic strategies in LC management.

Human ion channels (HICs) play a fundamental role in regulating cellular homeostasis, membrane potential, and signal transduction and have been increasingly reported in the pathophysiology of viral infections, including COVID-19 (6). Several studies have highlighted the dysregulation of HIC activity during SARS-CoV-2 infection, suggesting their involvement in COVID-19-associated complications (7), (8). They contribute to critical processes such as viral entry, replication, and host immune responses, thereby influencing disease progression and severity (9).

Among these, potassium channels constitute a major class of HICs that are essential for maintaining ionic balance, regulating membrane repolarization, and controlling cellular excitability across neuronal, cardiac, and epithelial systems (10), (11), (12), (13). Dysregulation of potassium channels is known to disrupt K^+ homeostasis and membrane potential, leading to altered neuronal signaling and impaired cellular function (14), (15), (13)**.** Hypokalemia, characterized by reduced serum potassium levels, is a serious condition that can lead to electrolyte imbalance, arrhythmias and seizures and has been frequently reported in patients with acute COVID-19 (16), (17). Notably, emerging case reports have documented persistent hypokalemia beyond the acute phase of infection, indicating sustained disruption of potassium homeostasis and a potential link to LC (17), (18). These channelopathies are associated with neuropsychiatric manifestations, cardiac abnormalities, and immune dysregulation and may also facilitate viral entry and persistence, highlighting their potential role in the multisystem nature of LC (19), (20), (21).

Moreover, due to their accessibility and functional significance, HICs have emerged as promising druggable targets (9). However, their specific role and regulatory dynamics in the context of LC remain largely unexplored.

Additionally, HICs, lipid metabolism and immune signaling pathways play critical roles in the host response to viral infections and the development of persistent disease states. Lipid metabolism is essential for viral replication, membrane remodeling, and energy homeostasis, while dysregulation of immune signaling pathways contributes to the chronic inflammation and prolonged symptomatology observed in LC (22), (23), (24). Emerging evidence suggests that these biological processes do not act independently but are highly interconnected, with significant cross-talk influencing disease progression (22), (23). However, the integrated interactions between HICs, lipid metabolism, and immune signaling pathways have not been systematically explored in LC. Understanding these interconnected molecular networks may provide deeper insights into the mechanisms underlying disease persistence.

Given the interconnected nature of these molecular processes, a systems-level approach is essential to comprehensively understand LC pathophysiology. Traditional differential expression analyses provide valuable insights into individual genes but often fail to capture the coordinated interactions between them. In contrast, gene co-expression network analysis enables the identification of functionally related gene modules and underlying regulatory patterns, offering a more holistic view of disease-associated molecular mechanisms (25). Such approaches may reveal key genes, thereby facilitating the identification of critical molecular drivers in LC.

With the lack of approved targeted therapies for LC, there is a need to identify effective treatment strategies. Drug repurposing offers a time- and cost-efficient approach by utilizing existing approved drugs with known safety profiles (26). Integrating transcriptomic findings with drug–target interaction data can facilitate the identification of potential therapeutic candidates by linking disease-associated molecular alterations to actionable targets (26), (27). Such strategies may accelerate the translation of molecular insights into clinical applications, providing a practical framework for the management of LC.

2 Methodology

2.1 Data Acquisition and Processing

RNA sequencing (RNA-Seq) data from 62 recovered COVID-19 recovered and 70 LC patients were obtained for this study. Two datasets (GSE251849 and GSE226260) were downloaded from the Gene Expression Omnibus database, whereas one dataset (PRJNA1184005) was acquired from NCBI's BioProject. A list of 493 HICs was downloaded from the HUGO Gene Nomenclature Committee database. Lipid metabolism-related genes (LMGs) were collected from the literature (28), (29), (30), (31), (32), (33), (34), (35), (36), (37), (38). Similarly, a list of immune signaling-related genes (ISGs) was obtained from the InnateDB (39). The quality of the RNA-Seq data was assessed using FastQC (v. 0.12.1) and further processed using Trimmomatic (v. 0.39) (40). Quality

filtered reads were aligned to the human genome GRCh38.p13 using STAR aligner (v. 2.7.11b) followed by gene expression quantification using HTSeq (v. 2.1.2) (41), (42). Batch effects arising from technical variability across samples were corrected using the ComBat function of the sva package (v. 3.54.0) prior to downstream analyses (43). The overall workflow is summarized in Figure 1.

2.2 Differential Expression and Functional Analysis

Differential gene expression analysis between COVID-19 recovered and LC gene expression profiles was performed using the DESeq2 package (v. 1.46.0) of R (R Foundation for Statistical Computing, Vienna, Austria) (44). Genes with a p value <= 0.05 and |log2fold change| > 0.6 were classified as differentially expressed genes (DEGs). A volcano plot was generated using the ggplot2 package (v. 3.5.2), with differentially expressed HICs, LMGs, and ISGs specifically labeled. Functional enrichment analysis for Gene Ontology (GO) and pathways was performed using the functions gseGO and gseKEGG, respectively, from ClusterProfiler (v. 4.14.6), an R package (45). Enriched terms and pathways up-regulated (activated) and down-regulated (suppressed) with a p value <=0.05 were visualized using R's dotplot function.

2.3 Network Construction and Pathway Analysis

Co-expression networks were constructed using the weighted gene co-expression network analysis (WGCNA) package (v. 1.74) of R (46). Expression profiles of DEGs were provided as an input and transformed using DESeq2's variance stabilizing transformation. To generate a scale-free topology network, a soft thresholding power of 4 was used. After converting expression data into a topological overlap matrix (TOM), the dynamic tree-cutting approach was used to detect initial modules. Modules were merged based on substantially similar expression profiles of the genes. Eigengene-trait correlation analysis was performed to identify modules significantly associated with COVID-19 recovered and LC. We used gene significance and module membership (MM) values to assess the correlation between gene expression profiles, module eigengenes, and binary characteristics. Gene significance versus MM plots was used to assess intramodular gene relationships (46). The most correlated modules were chosen, and the resulting networks were exported to Cytoscape with a weight threshold of 0.02 (47). Furthermore, pathways associated with the significant modules were identified using EnrichR (48).

2.4 Drug Interactions

Differentially expressed HICs and their subset in co-expression networks were considered potential druggable targets for drug repurposing. Approved drugs interacting with these HICs were identified using the Drug-Gene Interaction Database (49).

3 Results

3.1 Differential Gene Expression and Functional Enrichment

The analysis identified 715 DEGs, of which 266 were found to be down-regulated and 449 were up-regulated. Of the total DEGs, 18 were HICs, 22 were LMGs and 28 were ISGs (Figure 2). A list of DEGs is provided in Supplementary File 1. Furthermore, of the total differentially expressed HICs, 7 were potassium channels: *KCNA6, KCNG3, KCNH4, KCNJ10, KCNJ12, KCNN3,* and *KCTD4.* Table 1 represents the list of 7 deregulated potassium channels.

Functional enrichment analysis of DEGs led to the identification of 702 biological processes, 162 molecular functions, 77 cellular components, and 29 pathways to be enriched in LC patients (Figure 3) (Supplementary File 2). Pathways including antigen processing and presentation, complement and coagulation cascades, biosynthesis of unsaturated fatty acids, N-glycan biosynthesis, 2-oxocarboxylic acid metabolism, phagosome, and neuroactive ligand–receptor interaction were found to be suppressed in LC patients through their negative normalized enrichment score (NES). Similarly, pathways including type II diabetes mellitus, pancreatic secretion, and maturity onset diabetes of the young were found to be activated in LC patients through their positive NES.

3.2 Co-expression Network Analysis

Three significant co-expressed gene networks were identified using WGCNA, namely, the blue, brown, and turquoise modules, comprising 158, 98, and 79 DEGs, respectively (Figure 4 and Supplementary File 3).

The blue module comprised 5 HICs - chloride intracellular channel 6 (*CLIC6*), potassium voltage-gated channel subfamily A member 6 (*KCNA6*), potassium inwardly rectifying channel subfamily J member 10 (*KCNJ10*), potassium calcium-activated channel subfamily N member 3 (*KCNN3*), and potassium channel tetramerization domain containing 4 (*KCTD4*); 7 LMGs - adenylate cyclase 6 (*ADCY6*), cytochrome P450 family 27 subfamily A member 1 (*CYP27A1*), cytochrome P450 family 4 subfamily B member 1 (*CYP4B1*), diacylglycerol kinase kappa (*DGKK*), lipoprotein lipase (*LPL*), matrix metallopeptidase 1 (*MMP1*), and protein kinase cGMP-dependent 1 (*PRKG1*); and 10 ISGs - complement C1q B chain (*C1QB*), complement C1q C chain (*C1QC*), dedicator of cytokinesis 1 (*DOCK1*), interferon alpha inducible protein 27 (*IFI27*), immunoglobulin heavy constant gamma 1 (G1m marker) (*IGHG1*), immunoglobulin heavy constant gamma 2 (G2m marker) (*IGHG2*), leucine zipper tumor suppressor 1 (*LZTS1*), membrane spanning 4-domains A2 (*MS4A2*), programmed cell death 1 ligand 2 (*PDCD1LG2*), and vascular endothelial growth factor C (*VEGFC*) (Figure 5A). The blue module was further found to be associated with several pathways, including the phospholipase D signaling pathway, complement and coagulation cascades, cell adhesion molecule (CAM) interaction, efferocytosis, and peroxisome proliferator-activated receptor signaling pathway.

The brown module contained 2 HICs that included potassium voltage-gated channel subfamily H member 4 (*KCNH4*) and solute carrier family 22 member 10 (*SLC22A10*), 6 LMGs - calcium/calmodulin dependent protein kinase II alpha (*CAMK2A*), colony stimulating factor 1

(*CSF1*), C-X-C motif chemokine ligand 2 (*CXCL2*), dual specificity phosphatase 4 (*DUSP4*), SMAD family member 6 (*SMAD6*), ubiquitin specific peptidase 2 (*USP2*), and 6 ISGs - ATP binding cassette subfamily A member 1 (*ABCA1*), angiopoietin like 3 (*ANGPTL3*), angiopoietin like 4 (*ANGPTL4*), oxidized low density lipoprotein receptor 1 (*OLR1*), perilipin 5 (*PLIN5*), and prostaglandin E synthase (*PTGES*) (Figure 5B). The brown module was further found to be associated with pathways including viral protein interactions with cytokine and cytokine receptor, lipid and atherosclerosis, cholesterol metabolism, among others.

The turquoise module contained 1 LMG – adenylate cyclase 1 (*ADCY1*) and 1 ISG – C-C motif chemokine receptor 4 (*CCR4*) and was found to be associated with gap junctions through pathway analysis.

3.3 Drug-Target interactions

From the total differentially expressed HICs identified, 10 were found to interact with approved drugs (Supplementary File 4). Of these 10 HICs, KCNN3, KCNA6, and KCNJ10 were from the blue module, and KCNH4 was from the brown module. KCNN3 was observed to interact with dequalinium. KCNJ10 interacted with mitiglinide, glipizide, tolazamide, and chlorpropamide. Additionally, both KCNA6 and KCNH4 were found to interact with amifampridine, guanidine hydrochloride, dalfampridine, and amifampridine phosphate. (Figure 6).

4 Discussion

Given the latest definition of LC, the knowledge of mechanisms driving the condition and the multisystem nature of the symptoms experienced by the patients (50), (2), we performed a meta-analysis of transcriptomic data from COVID-19 recovered and LC patients to identify the underlying molecular alterations most likely responsible for these mechanisms.

Here, we identified DEGs in LC patients, including seven potassium ion channel genes, *KCNA6, KCNG3, KCNH4, KCNJ10, KCNJ12, KCNN3*, and *KCTD4,* among the differentially expressed HICs. Functional enrichment for the DEGs led to the identification of GO terms and pathways that may be altered in LC patients. Among the enriched Gene Ontology (GO) terms, 171 biological processes, 47 molecular functions, and 21 cellular components included differentially expressed HICs, LMGs, and ISGs. Functional enrichment led to the identification of GO terms and pathways that are activated and suppressed as a consequence of differential expression in LC patients. Pathways and processes related to diabetes and the nervous system were found to be activated, while several immune signaling, lipid metabolism, cell cycle, and other metabolic pathways were suppressed in LC patients, as revealed by pathway enrichment analysis. Furthermore, significant modules of highly correlated genes that were associated with pathways linked with LC were identified. Notably, these module-associated pathways were consistent with those identified through initial pathway enrichment analysis, suggesting that genes within these modules may contribute to LC pathophysiology. Furthermore, of the seven differentially expressed potassium channels, five (*KCNN3*, *KCNH4*, *KCNA6*, *KCNJ10*, and *KCTD4*) were found to be co-expressed

in the identified modules and finally, four of them (*KCNN3*, *KCNH4*, *KCNA6*, and *KCNJ10*) interacted with approved drugs.

KCNN3, belonging to the KCNN family of potassium channels, encodes a small conductance calcium-activated potassium channel (SK3). Functionally, SK3 mediates the voltage-independent transmembrane transfer of K^+ across the cell membrane through its interaction with calmodulin, which binds the intracellular calcium, allowing its opening (10). Due to its higher expression in the brain and heart, dysregulation of *KCNN3* is reported to be associated with neurological disorders and cardiac arrhythmia, which are also among the manifestations observed in LC (51), (19), (52), (53). Dysregulated *KCNN3* has also been reported in previous bioinformatic studies, suggesting their deeper investigation in LC-associated manifestations (54). SK3 is activated after membrane hyperpolarization, which then regulates neuronal excitability by contributing to the slow component of synaptic afterhyperpolarization (AHP). In up-regulated expression of *KCNN3*, as observed in our analysis, the increased regulatory effect of the channel would cause a delay in neuronal activation, which is often observed in several conditions, including schizophrenia and atrial fibrillation, a condition also associated with LC (55), (56). As a potential blocker of the SK3 channel, dequalinium prevents the slow reset period (AHP) followed by a nerve impulse, enhancing the excitability of a neuron (57), (55). Hence, the KCNN3-dequalinium interaction could provide a promising strategy in the management of neurological conditions observed in LC. In addition, we found it to interact with 21 DEGs, of which 1 was LMG - protein kinase CGMP-dependent 1 (*PRKG1*) and 2 were ISGs - immunoglobulin heavy constant gamma 1 (*IGHG1*) and programmed cell death 1 ligand 2 (*PDCD1LG2*). Of them, PDCD1LG2 has been reported as a major immune checkpoint during COVID-19 progression, while some have mentioned its elevation associated with T-cell exhaustion in LC cohorts (58), (59).

KCNA6 is a voltage-gated potassium channel that is highly expressed in the central nervous system, with the highest expression in the frontal and occipital cortex (13). It regulates neuronal excitability by mediating potassium ion transport, which is crucial for repolarizing neurons after action potentials (60). Mutations in *KCNA6* disrupt channel deactivation, leading to persistent neuronal excitability and early-onset epilepsy, leading to behavioral, cognitive, and psychiatric issues (13), (61). Additionally, exogenous expression of *KCNA6* was found to significantly increase spike-mediated pseudoviral entry (21). Notably, disrupting KCNA6 channel activity has been shown to decrease SARS-CoV-2 viral entry, highlighting it as a putative SARS-CoV-2 host factor (21). The upregulation of *KCNA6* identified in this study, along with its interaction with channel blocker drugs pose them as a potential molecule in LC-associated neurological manifestations.

KCNH4, located in the neocortex and the striatum, is a brain-specific gene that is associated with the regulation of neurotransmitter release, heart rate, insulin secretion, neuronal excitability, epithelial electrolyte transport, smooth muscle contraction, and cell volume (62). Dysregulation of *KCNH4* is reported to be associated with sleep regulation, neurodegeneration, and several neurodevelopmental disorders. Several studies have reported sleep disturbances in patients with a

history of acute COVID-19, suggesting that it is among the major neuropsychiatric symptoms experienced by patients (20), (63). Additionally, its interaction with *PTGES*, an LMG and 2 ISGs, *CAMK2A* and *DUSP4,* was revealed through co-expression analysis. These molecules, especially *CAMK2A* and *DUSP4,* have been reported to be linked with SARS-CoV-2 viral entry and LC-associated brain fog, respectively (64), (65). Furthermore, the upregulation of *KCNH4* and its interaction with channel blockers that were identified in this study suggest the therapeutic potential of KCNH4 in LC-associated neuropsychiatric symptoms.

Kir4.1, encoded by *KCNJ10*, is an inwardly rectifying potassium channel that maintains K^+ homeostasis in glial cells in the central nervous system, inner ear cells, and renal epithelial cells (11). Specifically, it is involved in stabilizing the resting membrane potential of astrocytes, clears extracellular K^+ to prevent neuronal over-excitation, and enables salt reabsorption in the kidney (12), (15). *KCNJ10* downregulation has been reported as a marker of astrocyte dysfunction in depression that may contribute to neuroinflammation-driven neuropsychiatric complications in LC (66). A decrease in *KCNJ10* contributes to loss of K^+ buffering capacity and disruption of ionic equilibrium in retinal Müller glial cells (15), (67). Additionally, disruption in channel functionality has been reported to cause EAST syndrome, making it critical in neurological implications (68). Furthermore, we identified *KCNJ10* interacting with *PDCD1LG2* through our analysis. The downregulation of *KCNJ10* in LC patients identified in this study and its association with neurological imbalance reported in the literature highlight its potential for studying neurological manifestations in LC.

All the findings of this study were derived through bioinformatic data analysis and data mining. It was primarily based on transcriptomic data, which captures gene expression patterns but does not directly verify protein-level changes or functional modifications in HICs, LMGs, and ISGs. The heterogeneity of LC progression across individuals and potential differences in underlying mechanisms may constrain the generalizability of the findings. Future studies incorporating longitudinal patient cohorts, electrophysiological measurements of HICs function, and functional assays in patient-derived cell and organoid models would not only strengthen these findings but also provide a more comprehensive understanding of the complex pathophysiology underlying LC.

5 Conclusion

Through comprehensive computational analysis and extensive data mining, we identified key DEGs, significantly co-expressed gene networks, and altered pathways associated with neurological, renal, and cardiovascular processes. Notably, the dysregulation and co-expression of HICs, particularly potassium channels, highlight their potential in LC symptom management. Collectively, these results suggest a critical subset of molecular alterations underlying broad multisystem dysregulation in LC and provide a molecular framework for understanding its pathophysiology, thereby facilitating the identification of potassium channels as potential targets.

However, further experimental validation in larger cohorts is necessary to confirm these observations and translate them into effective diagnostic and treatment strategies.

Conflict of Interest

The authors declare that they have no known competing financial interests or personal relationships that could have appeared to influence the work reported in this paper.

CRediT Authorship Contribution Statement

John P. George: Writing – review & editing, Writing – original draft, Visualization, Methodology, Investigation, Formal analysis, Data curation. Kiran Bharat Gaikwad: Writing – review & editing, Visualization, Investigation. Jyoti Sharma: Writing – review & editing, Supervision, Methodology, Investigation, Funding acquisition, Conceptualization.

Funding

This research did not receive any specific grant from funding agencies in the public, commercial, or not-for-profit sectors.

Acknowledgements

We would like to thank the authors of the manuscripts for making the datasets used in this study publicly available. J.S. would like to thank Council of Scientific and Industrial Research (CSIR), Government of India [37WS(0114)/2023-24/EMR-II/ASPIRE] and Indian Council of Medical Research (ICMR), Government of India [FIW-2025-01-00001091] for the research support. J.P.G. is supported by the CSIR [37WS(0114)/2023-24/EMR-II/ASPIRE] and K.B.G. is supported by the ICMR [FIW-2025-01-00001091]. J.S. was a recipient of the Bio-CARe Women Scientists award from the Department of Biotechnology (DBT), Government of India.

Data Availability Statement

The datasets used in this study are available in NCBI's Gene Expression Omnibus database (https://www.ncbi.nlm.nih.gov/geo/) and BioProject (https://www.ncbi.nlm.nih.gov/bioproject/). These datasets were derived using the following accessions - GSE251849, GSE226260, and PRJNA1184005.

Legends

FIGURE 1. *Overview of Workflow.* Publicly available transcriptomic data of COVID-19 recovered and long COVID was downloaded, processed, and treated for batch effect removal. Differential expression analysis was performed to identify differentially expressed genes. Functional enrichment for the identified differentially expressed genes (DEGs) was performed to identify associated Gene Ontology terms and pathways. Gene co-expression network analysis was performed to identify significant clusters comprising differentially expressed human ion channels (HICs) and lipid metabolism- and immune signaling-related genes. Approved drugs interacting with these critical HICs were identified. These drug-HICs interactions may provide potential strategies for drug repurposing.

FIGURE 2. *Volcano plot for differentially expressed genes*. Representation of differentially expressed genes identified using DESeq2. Blue points represent down-regulated genes. Red points represent up-regulated genes. Gray points represent genes with normal expression. Labels in the volcano plots represent differentially expressed human ion channels, lipid metabolism-, and immune signaling-related genes.

FIGURE 3. *Functional enrichment of differentially expressed genes*. A) Biological processes and B) pathways that were found to be activated and suppressed in long COVID patients.

FIGURE 4. *Weighted gene co-expression network analysis (WGCNA) of dysregulated genes in long COVID (LC).* (A) Scale independence plot depicting the relationship between soft threshold power (β=4) and scale-free topology fit. (B) Mean connectivity analysis illustrating how connectivity decreases with increasing soft threshold power. (C) Sample clustering dendrogram showing the relationship between COVID recovered and LC samples. (D) Module-trait relationship heatmap illustrating the correlation between identified modules and LC status, with red indicating a positive correlation and blue indicating a negative correlation. (E) Gene significance versus module membership plots for blue, brown and turquoise modules, demonstrating the relationship between gene significance for LC and intramodular connectivity.

FIGURE 5: *Co-expressed networks obtained through WGCNA:* (A) Blue module visualization with ion channels highlighted in orange nodes, LMGs highlighted in green nodes, and ISGs highlighted in pink nodes. This module includes genes associated with the phospholipase D signaling pathway, complement and coagulation cascades, cell adhesion molecule (CAM) interaction, efferocytosis, and peroxisome proliferator-activated receptor signaling pathway. (B) Brown module visualization with channels highlighted in orange nodes, LMGs highlighted in green nodes, and ISGs highlighted in pink nodes. This module was further found to be associated with pathways including viral protein interactions with cytokine and cytokine receptor, lipid and atherosclerosis, and cholesterol metabolism.

Figure 6: *Interactions between potassium channels and drugs:* (A) Potassium calcium-activated channel subfamily N member 3 (KCNN3) interacting with dequalinium. (B) Potassium voltage-

gated channel subfamily A member 6 (KCNA6) interacting with amifampridine (3,4-DAP), guanidine hydrochloride (GuHCl), dalfampridine (4-AP), and amifampridine phosphate (3,4-DAP). (C) Potassium inwardly rectifying channel subfamily J member 10 (KCNJ10) is known to interact with mitiglinide (MGN), glipizide (GZ), tolazamide (TOL), and chlorpropamide. (D) Potassium voltage-gated channel subfamily H member 4 (KCNH4) is known to interact with Amifampridine (3,4-DAP), guanidine hydrochloride (GuHCl), dalfampridine (4-AP), and amifampridine phosphate (3,4-DAP).

Supplementary File 1. Differential gene expression analysis results generated using DESeq2.

Supplementary File 2. Functional enrichment analysis results obtained using ClusterProfiler and Enrichr.

Supplementary File 3. Node and edge information for the three significant WGCNA modules (Blue, Brown, and Turquoise).

Supplementary File 4. Drug interacting with the identified differentially expressed human ion channels retrieved from the Drug-Gene Interaction Database.

371 **Table 1: Deregulated potassium ion channels in LC patients.** List of seven up- and down-
372 regulated potassium channels in LC patients with their corresponding description,
373 log2Foldchange, significant p value, and dysregulation status

Potassium channels	**Description**	**log2FC**	***p* value**	**Dysregulation**
KCNH4	Potassium voltage-gated channel subfamily H member 4	1.29209	3.59E-06	Up-regulated
KCNJ12	Potassium inwardly rectifying channel subfamily J member 12	1.67679	0.00191	Up-regulated
KCNG3	Potassium voltage-gated channel modifier subfamily G member 3	1.78694	0.03089	Up-regulated
KCNN3	Potassium calcium-activated channel subfamily N member 3	0.65056	0.03441	Up-regulated
KCNA6	Potassium voltage-gated channel subfamily A member 6	0.81391	0.04806	Up-regulated
KCNJ10	Potassium inwardly rectifying channel subfamily J member 10	-1.26974	0.00116	Down-regulated
KCTD4	Potassium channel tetramerization domain containing 4	-1.05143	0.03132	Down-regulated

374

375

376

377

378

References

1. Hou Y, Gu T, Ni Z, Shi X, Ranney ML, Mukherjee B. Global Prevalence of Long COVID, its Subtypes and Risk factors: An Updated Systematic Review and Meta-Analysis. medRxiv. 2025.
2. Davis HE, McCorkell L, Vogel JM, Topol EJ. Long COVID: major findings, mechanisms and recommendations. Nat Rev Microbiol. 2023;21(3):133-46.
3. Yang X, Rutkovsky AC, Zhou J, Zhong Y, Reese J, Schnell T, et al. Characterization of Altered Gene Expression and Histone Methylation in Peripheral Blood Mononuclear Cells Regulating Inflammation in COVID-19 Patients. J Immunol. 2022;208(8):1968-77.
4. Zhang JY, Whalley JP, Knight JC, Wicker LS, Todd JA, Ferreira RC. SARS-CoV-2 infection induces a long-lived pro-inflammatory transcriptional profile. Genome Med. 2023;15(1):69.
5. Gomez-Carballa A, Pischedda S, Pardo-Seco J, Gomez-Rial J, Martinon-Torres F, Salas A. Interferon gene expression declines over time post-COVID infection and in long COVID patients. Infect Dis (Lond). 2025;57(1):35-48.
6. Charlton FW, Pearson HM, Hover S, Lippiat JD, Fontana J, Barr JN, et al. Ion Channels as Therapeutic Targets for Viral Infections: Further Discoveries and Future Perspectives. Viruses. 2020;12(8).
7. John P. George, K. T. Shreya Parthasarathi, Kiran Bharat Gaikwad, Shweta Rana, Vibha Gupta, Punit Kaur, et al. Identifying the interactome of altered ion channels with lipid metabolism in SARS-CoV-2 infected patients in post-COVID-19 era. 2024.
8. Munjal NS, Sapra D, Parthasarathi KTS, Goyal A, Pandey A, Banerjee M, et al. Deciphering the Interactions of SARS-CoV-2 Proteins with Human Ion Channels Using Machine-Learning-Based Methods. Pathogens. 2022;11(2).
9. Russell T, Gangotia D, Barry G. Assessing the potential of repurposing ion channel inhibitors to treat emerging viral diseases and the role of this host factor in virus replication. Biomed Pharmacother. 2022;156:113850.
10. Weatherall KL, Goodchild SJ, Jane DE, Marrion NV. Small conductance calcium-activated potassium channels: from structure to function. Prog Neurobiol. 2010;91(3):242-55.
11. Scholl UI, Choi M, Liu T, Ramaekers VT, Hausler MG, Grimmer J, et al. Seizures, sensorineural deafness, ataxia, mental retardation, and electrolyte imbalance (SeSAME syndrome) caused by mutations in KCNJ10. Proc Natl Acad Sci U S A. 2009;106(14):5842-7.
12. Zhang H, Zhu L, Wang F, Wang R, Hong Y, Chen Y, et al. Novel KCNJ10 Compound Heterozygous Mutations Causing EAST/SeSAME-Like Syndrome Compromise Potassium Channel Function. Front Genet. 2019;10:912.
13. Salpietro V, Galassi Deforie V, Efthymiou S, O'Connor E, Marce-Grau A, Maroofian R, et al. De novo KCNA6 variants with attenuated K(V) 1.6 channel deactivation in patients with epilepsy. Epilepsia. 2023;64(2):443-55.
14. Abbasian V, Davoudi S, Vahabzadeh A, Maftoon-Azad MJ, Janahmadi M. Astroglial Kir4.1 and AQP4 Channels: Key Regulators of Potassium Homeostasis and Their Implications in Autism Spectrum Disorders. Cell Mol Neurobiol. 2025;45(1):56.
15. Su XT, Wang WH. The expression, regulation, and function of Kir4.1 (Kcnj10) in the mammalian kidney. Am J Physiol Renal Physiol. 2016;311(1):F12-5.
16. Alfano G, Ferrari A, Fontana F, Perrone R, Mori G, Ascione E, et al. Hypokalemia in Patients with COVID-19. Clin Exp Nephrol. 2021;25(4):401-9.
17. Alnafiey MO, Alangari AM, Alarifi AM, Abushara A. Persistent Hypokalemia post SARS-coV-2 infection, is it a life-long complication? Case report. Ann Med Surg (Lond). 2021;62:358-61.
18. Albashash H. Persistent Hypokalemia: A Manifestation of Long COVID Syndrome? Journal of the American Society of Nephrology. 2025;36.
19. Mahida S, Mills RW, Tucker NR, Simonson B, Macri V, Lemoine MD, et al. Overexpression of KCNN3 results in sudden cardiac death. Cardiovasc Res. 2014;101(2):326-34.

20. Davis HE, Assaf GS, McCorkell L, Wei H, Low RJ, Re'em Y, et al. Characterizing long COVID in an international cohort: 7 months of symptoms and their impact. EClinicalMedicine. 2021;38:101019.
21. Dinesh RK, Wang C, Qu Y, Rustagi A, Cousins H, Zengel J, et al. Membrane-wide screening identifies potential tissue-specific determinants of SARS-CoV-2 tropism. PLoS Pathog. 2025;21(7):e1013157.
22. Caterino M, Gelzo M, Sol S, Fedele R, Annunziata A, Calabrese C, et al. Dysregulation of lipid metabolism and pathological inflammation in patients with COVID-19. Sci Rep. 2021;11(1):2941.
23. Lee W, Ahn JH, Park HH, Kim HN, Kim H, Yoo Y, et al. COVID-19-activated SREBP2 disturbs cholesterol biosynthesis and leads to cytokine storm. Signal Transduct Target Ther. 2020;5(1):186.
24. Pavon R, Parra S, Rubio FJ, Feliu M, Rios M, Iftimie S, et al. Assessment of physical status and analysis of lipidomic and metabolomic alterations in patients with Post-COVID-19 condition. PLoS One. 2026;21(3):e0341192.
25. van Dam S, Vosa U, van der Graaf A, Franke L, de Magalhaes JP. Gene co-expression analysis for functional classification and gene-disease predictions. Brief Bioinform. 2018;19(4):575-92.
26. Saranraj K, Kiran PU. Drug repurposing: Clinical practices and regulatory pathways. Perspect Clin Res. 2025;16(2):61-8.
27. Savander S, Curabaz NN, Abbasi AM, Khan A, Saeed K, Tanoli Z. Data-driven strategies for drug repurposing: insights, recommendations, and case studies. Brief Bioinform. 2025;26(6).
28. Li J, Li Q, Su Z, Sun Q, Zhao Y, Feng T, et al. Lipid metabolism gene-wide profile and survival signature of lung adenocarcinoma. Lipids Health Dis. 2020;19(1):222.
29. Fernandez LP, Gomez de Cedron M, Ramirez de Molina A. Alterations of Lipid Metabolism in Cancer: Implications in Prognosis and Treatment. Front Oncol. 2020;10:577420.
30. Dunn TM, Tifft CJ, Proia RL. A perilous path: the inborn errors of sphingolipid metabolism. J Lipid Res. 2019;60(3):475-83.
31. Moskot M, Jakobkiewicz-Banecka J, Smolinska E, Banecki B, Wegrzyn G, Gabig-Ciminska M. Activities of genes controlling sphingolipid metabolism in human fibroblasts treated with flavonoids. Metab Brain Dis. 2015;30(5):1257-67.
32. Meng Q, Hu X, Zhao X, Kong X, Meng YM, Chen Y, et al. A circular network of coregulated sphingolipids dictates lung cancer growth and progression. EBioMedicine. 2021;66:103301.
33. El-Fasakhany FM, Uchimura K, Kannagi R, Muramatsu T. A novel human Gal-3-O-sulfotransferase: molecular cloning, characterization, and its implications in biosynthesis of (SO(4)-3)Galbeta1-4(Fucalpha1-3)GlcNAc. J Biol Chem. 2001;276(29):26988-94.
34. Russo A, Biselli-Chicote PM, Kawasaki-Oyama RS, Castanhole-Nunes MMU, Maniglia JV, de Santi Neto D, et al. Differential Expression of Prostaglandin I2 Synthase Associated with Arachidonic Acid Pathway in the Oral Squamous Cell Carcinoma. J Oncol. 2018;2018:6301980.
35. Lutz CS, Cornett AL. Regulation of genes in the arachidonic acid metabolic pathway by RNA processing and RNA-mediated mechanisms. Wiley Interdiscip Rev RNA. 2013;4(5):593-605.
36. Astudillo AM, Balgoma D, Balboa MA, Balsinde J. Dynamics of arachidonic acid mobilization by inflammatory cells. Biochim Biophys Acta. 2012;1821(2):249-56.
37. Sonnweber T, Pizzini A, Nairz M, Weiss G, Tancevski I. Arachidonic Acid Metabolites in Cardiovascular and Metabolic Diseases. Int J Mol Sci. 2018;19(11).
38. Hanna VS, Hafez EAA. Synopsis of arachidonic acid metabolism: A review. J Adv Res. 2018;11:23-32.
39. Breuer K, Foroushani AK, Laird MR, Chen C, Sribnaia A, Lo R, et al. InnateDB: systems biology of innate immunity and beyond--recent updates and continuing curation. Nucleic Acids Res. 2013;41(Database issue):D1228-33.
40. Bolger AM, Lohse M, Usadel B. Trimmomatic: a flexible trimmer for Illumina sequence data. Bioinformatics. 2014;30(15):2114-20.
41. Dobin A, Davis CA, Schlesinger F, Drenkow J, Zaleski C, Jha S, et al. STAR: ultrafast universal RNA-seq aligner. Bioinformatics. 2013;29(1):15-21.

42. Anders S, Pyl PT, Huber W. HTSeq--a Python framework to work with high-throughput sequencing data. Bioinformatics. 2015;31(2):166-9.
43. Leek JT, Johnson WE, Parker HS, Jaffe AE, Storey JD. The sva package for removing batch effects and other unwanted variation in high-throughput experiments. Bioinformatics. 2012;28(6):882-3.
44. Anders S, Huber W. Differential expression analysis for sequence count data. Genome Biol. 2010;11(10):R106.
45. Yu G, Wang LG, Han Y, He QY. clusterProfiler: an R package for comparing biological themes among gene clusters. OMICS. 2012;16(5):284-7.
46. Langfelder P, Horvath S. WGCNA: an R package for weighted correlation network analysis. BMC Bioinformatics. 2008;9:559.
47. Shannon P, Markiel A, Ozier O, Baliga NS, Wang JT, Ramage D, et al. Cytoscape: a software environment for integrated models of biomolecular interaction networks. Genome Res. 2003;13(11):2498-504.
48. Chen EY, Tan CM, Kou Y, Duan Q, Wang Z, Meirelles GV, et al. Enrichr: interactive and collaborative HTML5 gene list enrichment analysis tool. BMC Bioinformatics. 2013;14:128.
49. Cannon M, Stevenson J, Stahl K, Basu R, Coffman A, Kiwala S, et al. DGIdb 5.0: rebuilding the drug-gene interaction database for precision medicine and drug discovery platforms. Nucleic Acids Res. 2024;52(D1):D1227-D35.
50. Ely EW, Brown LM, Fineberg HV, National Academies of Sciences E, Medicine Committee on Examining the Working Definition for Long C. Long Covid Defined. N Engl J Med. 2024;391(18):1746-53.
51. Cox HC, Lea RA, Bellis C, Carless M, Dyer T, Blangero J, et al. Variants in the human potassium channel gene (KCNN3) are associated with migraine in a high risk genetic isolate. J Headache Pain. 2011;12(6):603-8.
52. Leonel JW, Ciurleo GCV, Formiga AM, Vasconcelos TMF, de Andrade MH, Feitosa WLQ, et al. Long COVID: neurological manifestations - an updated narrative review. Dement Neuropsychol. 2024;18:e20230076.
53. Huseynov A, Akin I, Duerschmied D, Scharf RE. Cardiac Arrhythmias in Post-COVID Syndrome: Prevalence, Pathology, Diagnosis, and Treatment. Viruses. 2023;15(2).
54. Zhang H, Feng T. Network-Based Data Analysis Reveals Ion Channel-Related Gene Features in COVID-19: A Bioinformatic Approach. Biochem Genet. 2023;61(2):471-505.
55. Soden ME, Jones GL, Sanford CA, Chung AS, Guler AD, Chavkin C, et al. Disruption of dopamine neuron activity pattern regulation through selective expression of a human KCNN3 mutation. Neuron. 2013;80(4):997-1009.
56. Kanuri SH, Jayesh Sirrkay P, Ulucay AS. COVID-19 HEART unveiling as atrial fibrillation: pathophysiology, management and future directions for research. Egypt Heart J. 2023;75(1):36.
57. Imbrici P, Camerino DC, Tricarico D. Major channels involved in neuropsychiatric disorders and therapeutic perspectives. Front Genet. 2013;4:76.
58. Zhang X, Chen B, Liu K, Ma Y, Liu Y, Zhou H, et al. Infection with COVID-19 promotes the progression of pancreatic cancer through the PI3K-AKT signaling pathway. Discov Oncol. 2023;14(1):225.
59. Li C, Yue L, Ju Y, Wang J, Lu H, Li L, et al. Transcriptomic analysis for the retested positive COVID-19 patients with long-term persistent SARS-CoV-2 but without symptoms in Wuhan. Clin Transl Med. 2023;13(1):e1172.
60. UniProt Knowledgebase [Available from: https://www.uniprot.org/uniprotkb/.
61. Tsai MH, Lo CH, Liu YX, Wu SN, Kuo CY, Liu YH, et al. De novo missense variants of KCNA3, KCNA4, and KCNA6 cause early onset developmental epileptic encephalopathy. Hum Mol Genet. 2025;34(16):1392-404.
62. NCBI Gene [Available from: https://www.ncbi.nlm.nih.gov/gene/.
63. Tedjasukmana R, Budikayanti A, Islamiyah WR, Witjaksono A, Hakim M. Sleep disturbance in post COVID-19 conditions: Prevalence and quality of life. Front Neurol. 2022;13:1095606.

64. Wenzhong L, Hualan L. COVID-19: the CaMKII-like system of S protein drives membrane fusion and induces syncytial multinucleated giant cells. Immunol Res. 2021;69(6):496-519.
65. Harb H. Treg cell epigenetic modifications controlling Brain fog in Long COVID 9015. The Journal of Immunology. 2025;214.
66. Costanza A, Amerio A, Aguglia A, Rossi M, Parise A, Magnani L, et al. Reactive Astrocytosis-A Potential Contributor to Increased Suicide in Long COVID-19 Patients? Brain Sci. 2024;14(10).
67. Mesentier-Louro LA, Rangel B, Stell L, Shariati MA, Dalal R, Nathan A, et al. Hypoxia-induced inflammation: Profiling the first 24-hour posthypoxic plasma and central nervous system changes. PLoS One. 2021;16(3):e0246681.
68. Reichold M, Zdebik AA, Lieberer E, Rapedius M, Schmidt K, Bandulik S, et al. KCNJ10 gene mutations causing EAST syndrome (epilepsy, ataxia, sensorineural deafness, and tubulopathy) disrupt channel function. Proc Natl Acad Sci U S A. 2010;107(32):14490-5.

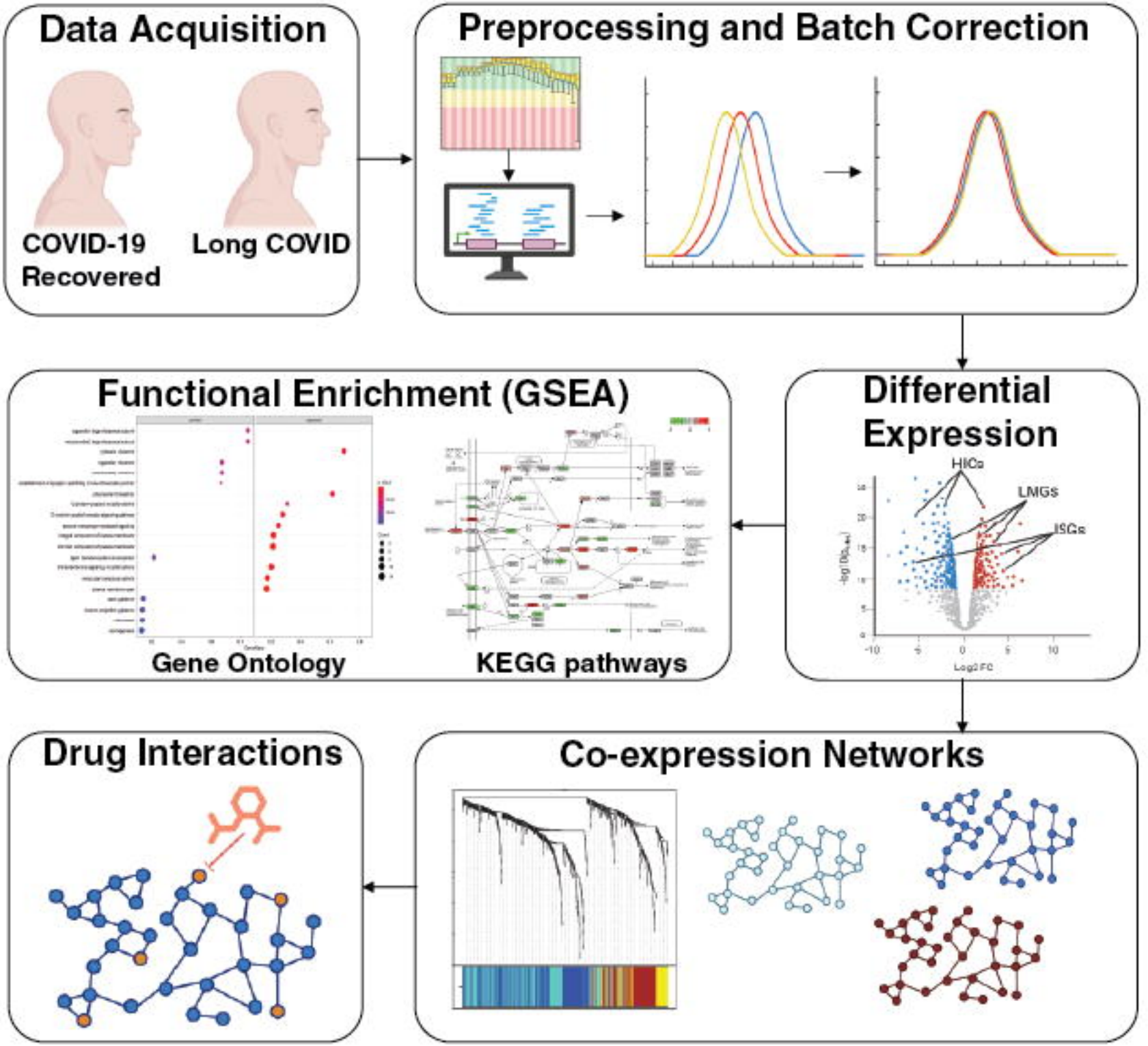
Data Acquisition
COVID-19 Recovered
Long COVID
Preprocessing and Batch Correction
Functional Enrichment (GSEA)
Gene Ontology
KEGG pathways
Differential Expression
HICs
LMGs
ISGs
Log2 FC
Drug Interactions
Co-expression Networks

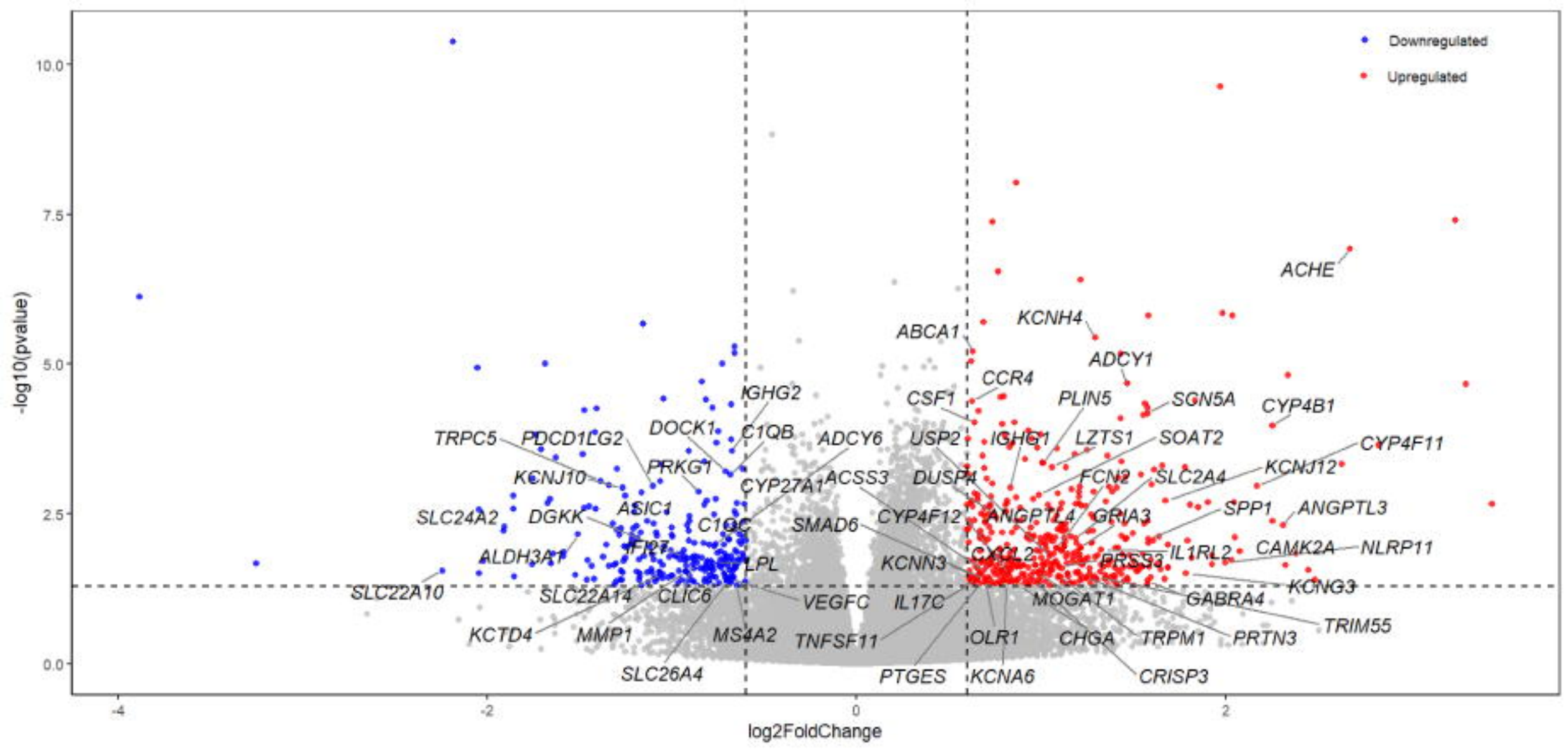
Downregulated
Upregulated
-log10(pvalue)
log2FoldChange
10.0
7.5
5.0
2.5
0.0
-4
-2
0
2
ACHE
KCNH4
ABCA1
ADCY1
CCR4
CSF1
PLIN5
SGN5A
CYP4B1
IGHG2
DOCK1
C1QB
ADCY6
USP2
IGHG1
LZTS1
SOAT2
CYP4F11
TRPC5
PDCD1LG2
PRKG1
KCNJ10
CYP27A1
ACSS3
DUSP4
FCN2
SLC2A4
KCNJ12
SLC24A2
DGKK
ASIC1
C1QC
SMAD6
CYP4F12
ANGPTL4
GRIA3
SPP1
ANGPTL3
ALDH3A1
IFI27
LPL
KCNN3
CXCL2
PRSS33
IL1RL2
CAMK2A
NLRP11
SLC22A10
SLC22A14
CLIC6
VEGFC
IL17C
MOGAT1
GABRA4
KCNG3
KCTD4
MMP1
MS4A2
TNFSF11
OLR1
CHGA
TRPM1
PRTN3
TRIM55
SLC26A4
PTGES
KCNA6
CRISP3

A

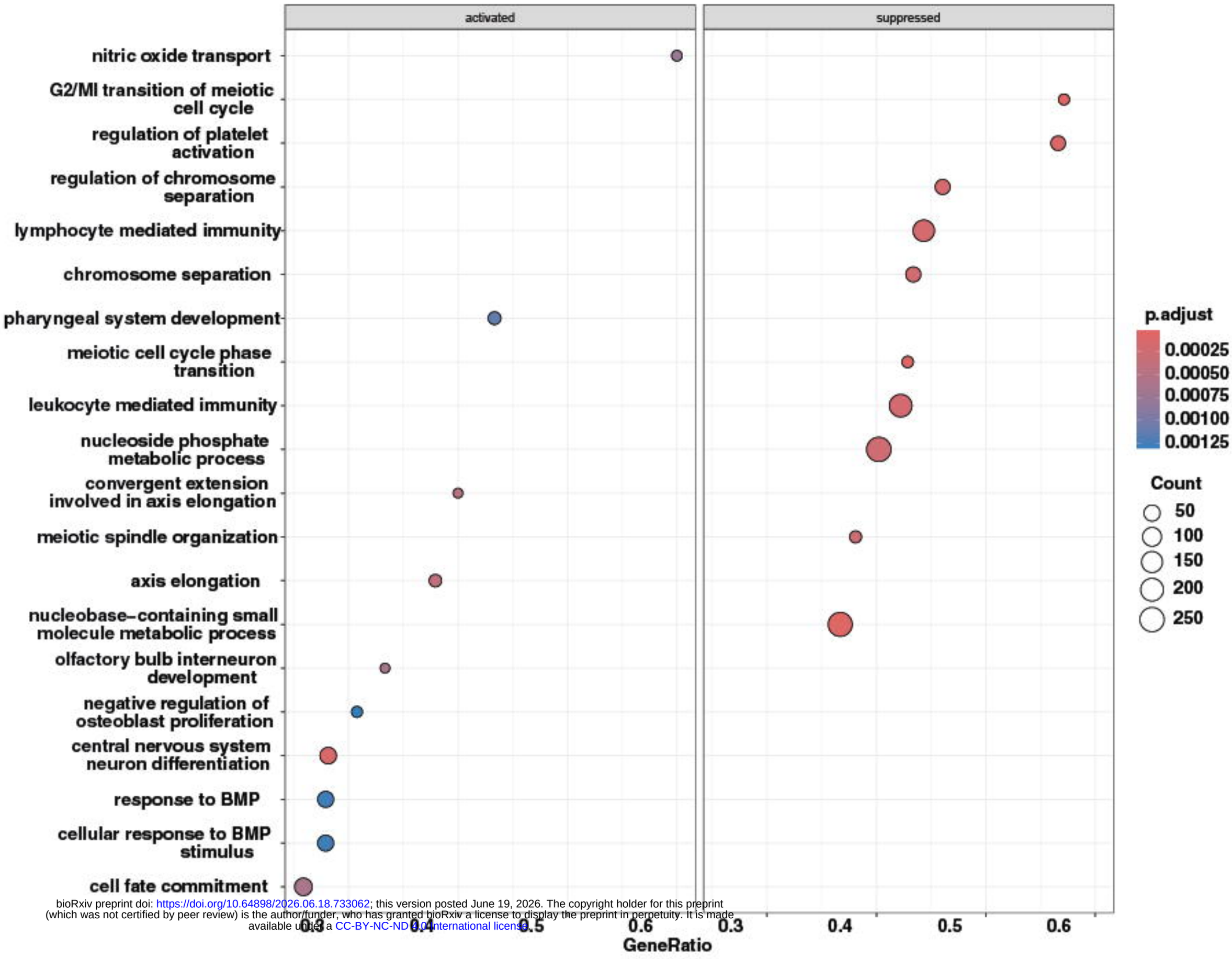

B

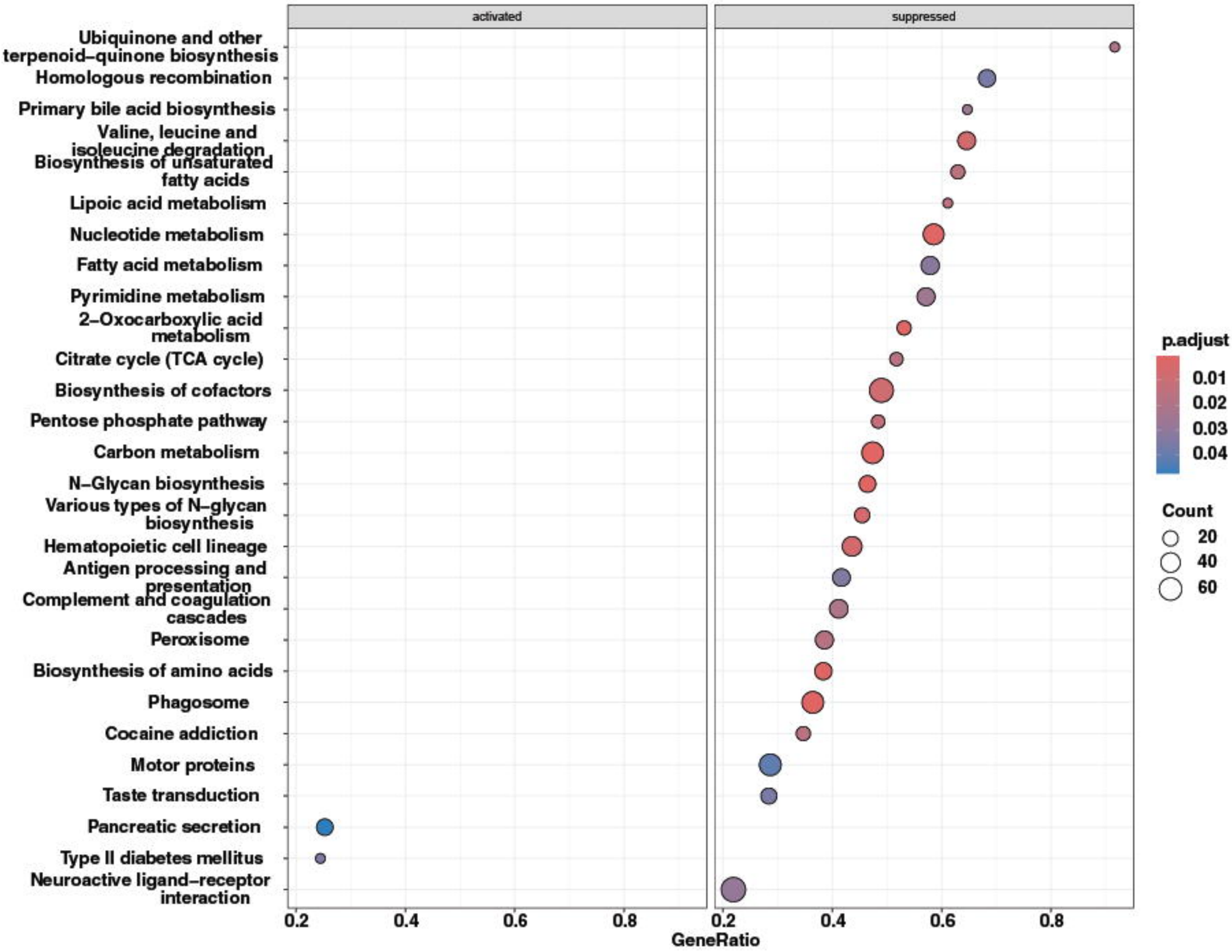

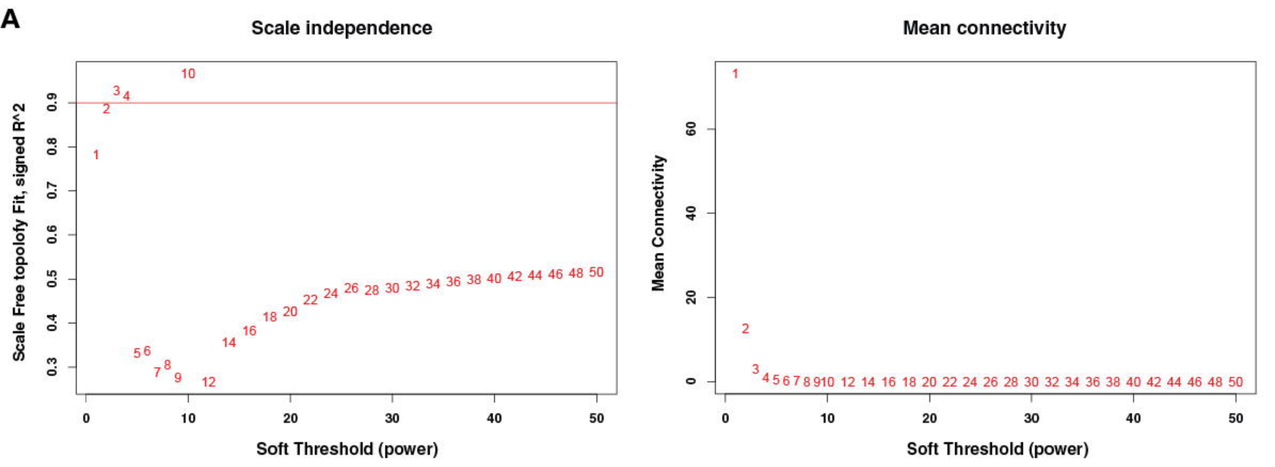

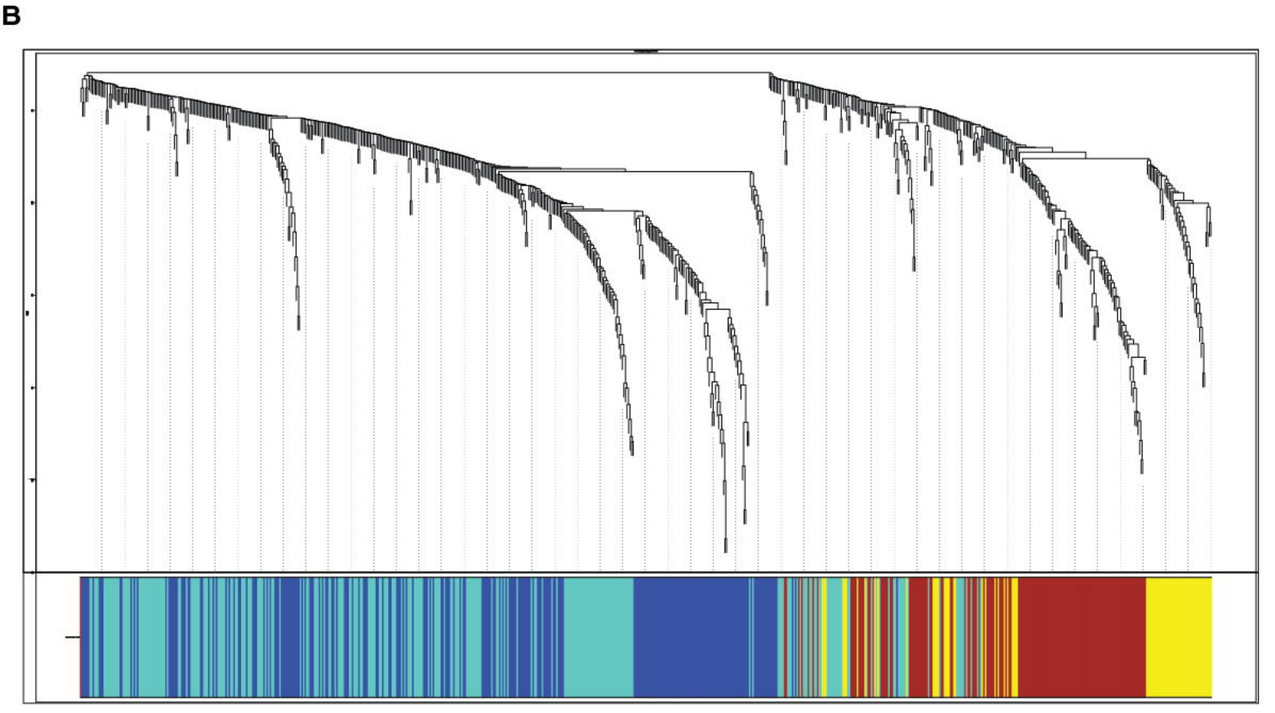

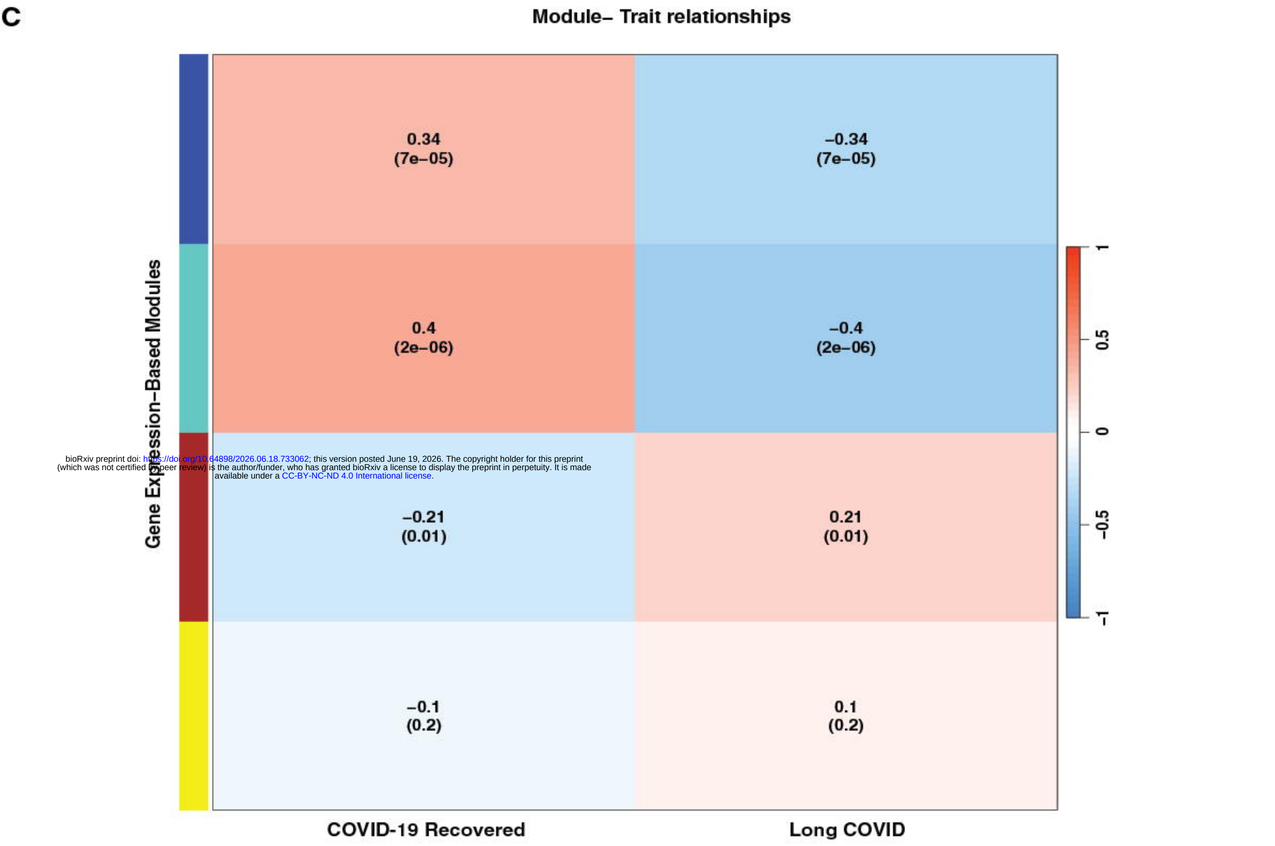

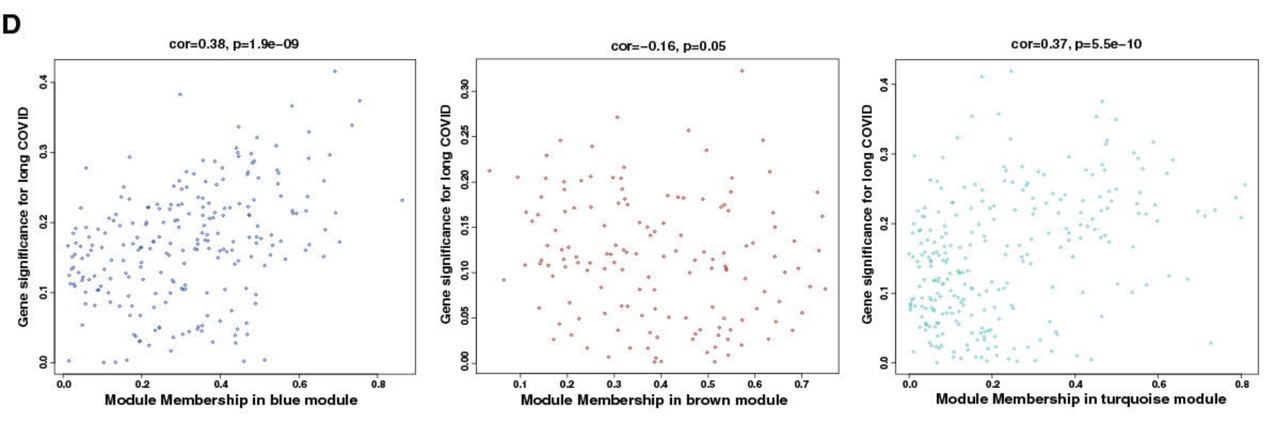

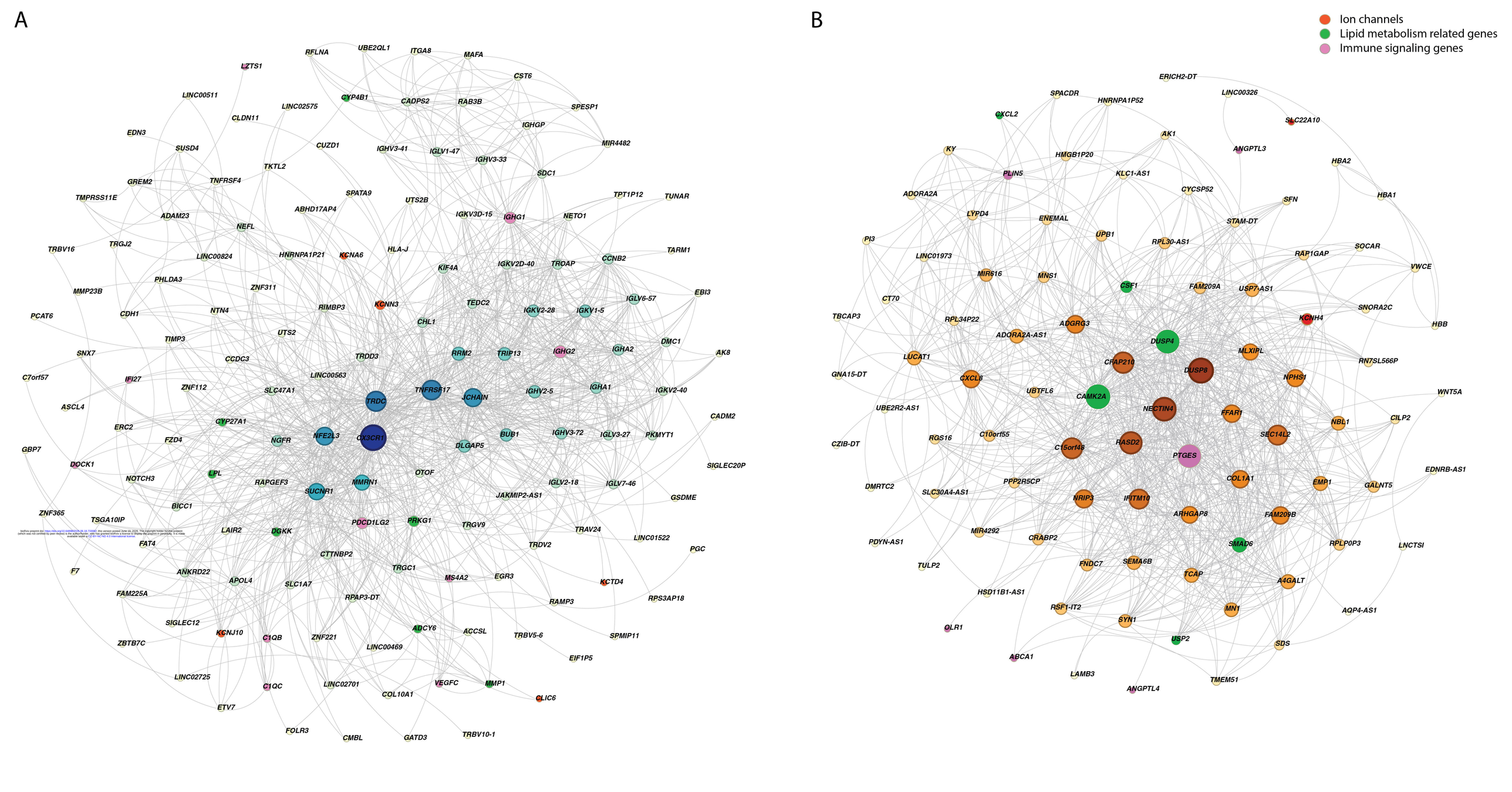
A
B
Ion channels
Lipid metabolism related genes
Immune signaling genes
RFLNA
UBE2QL1
ITGA8
MAFA
LZTS1
CST6
LINC00511
CYP4B1
CADPS2
RAB3B
SPESP1
LINC02575
CLDN11
IGHGP
EDN3
SUSD4
CUZD1
IGHV3-41
IGLV1-47
MIR4482
IGHV3-33
TKTL2
SDC1
GREM2
TNFRSF4
TMPRSS11E
SPATA9
UTS2B
TPT1P12
TUNAR
ABHD17AP4
ADAM23
IGKV3D-15
IGHG1
NETO1
NEFL
TRBV16
TRGJ2
LINC00824
HNRNPA1P21
KCNA6
HLA-J
TARM1
KIF4A
IGKV2D-40
TROAP
CCNB2
PHLDA3
MMP23B
ZNF311
EBI3
IGLV6-57
CDH1
NTN4
RIMBP3
KCNN3
TEDC2
IGKV2-28
IGKV1-5
PCAT6
CHL1
UTS2
TIMP3
DMC1
SNX7
CCDC3
TRDD3
RRM2
TRIP13
IGHG2
IGHA2
AK8
C7orf57
IFI27
LINC00563
ZNF112
SLC47A1
TNFRSF17
JCHAIN
IGHV2-5
IGHA1
IGKV2-40
TRDC
ASCL4
CADM2
CYP27A1
ERC2
NFE2L3
CX3CR1
BUB1
IGHV3-72
IGLV3-27
PKMYT1
FZD4
NGFR
DLGAP5
GBP7
SIGLEC20P
DOCK1
OTOF
LPL
NOTCH3
RAPGEF3
MMRN1
IGLV2-18
IGLV7-46
SUCNR1
JAKMIP2-AS1
GSDME
BICC1
ZNF365
TSGA10IP
PDCD1LG2
PRKG1
TRGV9
LAIR2
DGKK
TRAV24
LINC01522
FAT4
TRDV2
PGC
CTTNBP2
F7
ANKRD22
TRGC1
MS4A2
EGR3
KCTD4
APOL4
SLC1A7
FAM225A
RPAP3-DT
RAMP3
RPS3AP18
SIGLEC12
KCNJ10
ADCY6
ACCSL
TRBV5-6
SPMIP11
ZBTB7C
C1QB
ZNF221
LINC00469
EIF1P5
LINC02725
C1QC
LINC02701
VEGFC
MMP1
CLIC6
COL10A1
ETV7
FOLR3
CMBL
GATD3
TRBV10-1
ERICH2-DT
SPACDR
HNRNPA1P52
LINC00326
CXCL2
SLC22A10
AK1
KY
HMGB1P20
ANGPTL3
HBA2
PLIN5
KLC1-AS1
ADORA2A
CYCSP52
HBA1
SFN
LYPD4
ENEMAL
STAM-DT
PI3
UPB1
RPL30-AS1
SOCAR
LINC01973
RAP1GAP
VWCE
MIR616
MNS1
CSF1
FAM209A
USP7-AS1
CT70
SNORA2C
TBCAP3
RPL34P22
ADGRG3
KCNH4
HBB
ADORA2A-AS1
DUSP4
MLXIPL
LUCAT1
CRAP210
DUSP8
RN7SL566P
GNA15-DT
CXCL8
NPHS1
UBTFL6
CAMK2A
WNT5A
UBE2R2-AS1
NECTIN4
FFAR1
NBL1
CILP2
CZIB-DT
RGS16
C10orf55
RASD2
SEC14L2
C15orf48
PTGES
EDNRB-AS1
DMRTC2
PPP2R5CP
COL1A1
EMP1
GALNT5
SLC30A4-AS1
NRIP3
IFITM10
ARHGAP8
FAM209B
MIR4292
PDYN-AS1
CRABP2
SMAD6
RPLP0P3
LNCTSI
TULP2
FNDC7
SEMA6B
TCAP
A4GALT
HSD11B1-AS1
RSF1-IT2
MN1
AQP4-AS1
SYN1
OLR1
USP2
SDS
ABCA1
LAMB3
TMEM51
ANGPTL4

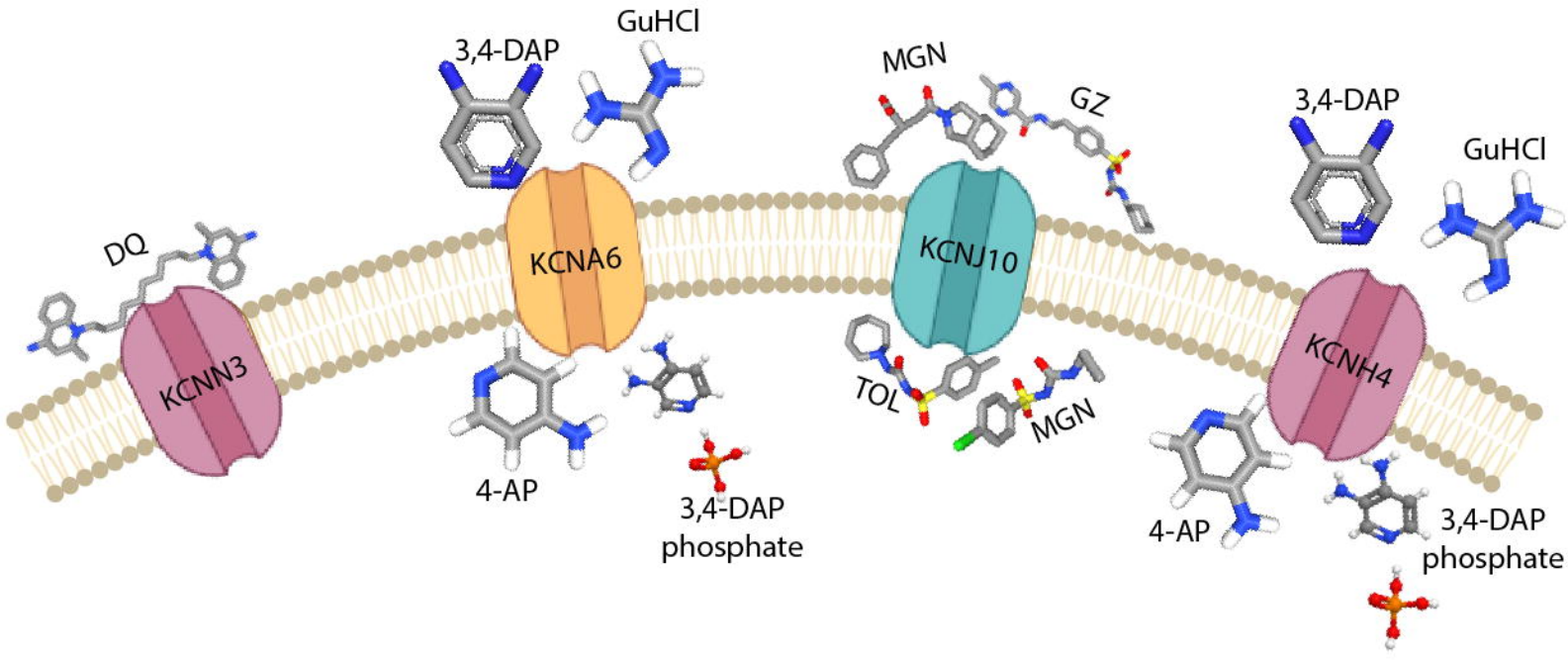
DQ
KCNN3
3,4-DAP
GuHCl
KCNA6
4-AP
3,4-DAP
phosphate
MGN
GZ
KCNJ10
TOL
MGN
3,4-DAP
GuHCl
KCNH4
4-AP
3,4-DAP
phosphate